Supplementary Information for

Ultra-Low Lattice Thermal Conductivity and Thermoelectric Performance in Monolayer Mg_3As_2 and Mg_3SbAs

Tao Yu, Xi-Long Dou*, Ya-Hui Li, Si-Zhuo Qiu, Ting Song, Xiao-Wei Sun*

School of Mathematics and Physics, Lanzhou Jiaotong University, Lanzhou 730070, China

The monolayer Mg_3SbAs structure exists in two possible configurations. In Mg_3SbAs (1), Sb atoms occupy (0.333, 0.666, 0.375) and As atoms occupy (0.666, 0.333, 0.581); in Mg_3SbAs (2), Sb atoms occupy (0.666, 0.333, 0.588) and As atoms occupy (0.333, 0.666, 0.380). We calculated their formation energies and selected the one with lower formation energy, Mg_3SbAs (1), for subsequent calculations.

Table S1 Mg_3As_2, Mg_3SbAs (1), and Mg_3SbAs (2) formation energies

Matter	Formation Energies
Mg_3As_2	-1.6819532484 eV
$Mg_3SbAs(1)$	-1.1946123617 eV
$Mg_3SbAs(2)$	-0.8860788117 eV

To clarify the effect of SOC on the electronic structures of Mg_3As_2 and Mg_3SbAs, we calculated the band structures with SOC.The results indicate that while the inclusion of SOC induces band splitting and a further reduction in the band gap, it does not significantly alter the overall band structure, particularly the conduction band minimum (CBM).

Fig. S1 Band structures of (a) Mg_3As_2 and (b) Mg_3SbAs calculated using SOC

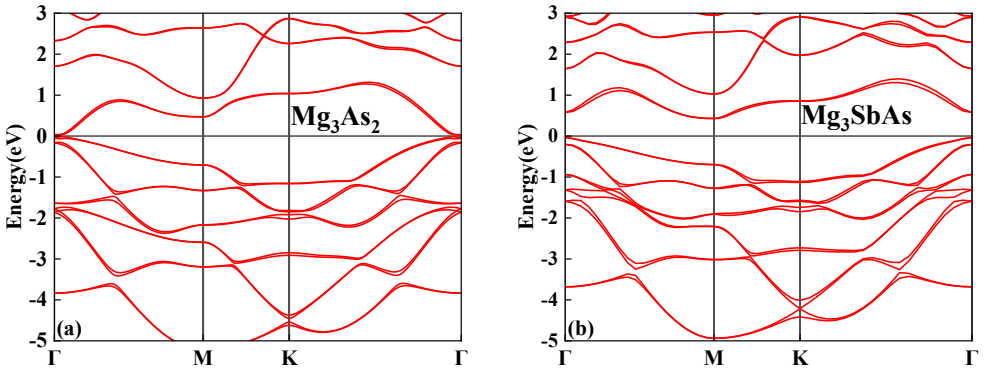

To evaluate the mechanical stability of monolayer Mg_3As_2 and Mg_3SbAs, we investigated mechanical stability using the finite distortion method.

Table S2 Elastic Constants of Mg_3As_2 and Mg_3SbAs

Matter	C_{11} (GPa)	C_{12} (GPa)	C_{66} (GPa)
Mg_3As_2	65.2649	34.8569	15.2040
Mg_3SbAs	60.8533	23.4988	18.6773

Calculations indicate that monolayer Mg_3As_2 and Mg_3SbAs satisfy the mechanical stability criteria. To further evaluate the stability of these structures, we performed ab initio molecular dynamics (AIMD) simulations at temperatures ranging from 300 to 900 K using the Nosé-Hoover thermostat. A 4 × 4 × 1 supercell was employed to mitigate artificial interactions arising from periodic boundary conditions, with a time step of 1 fs and a total duration of 5 ps. As depicted in Fig. S2, the structure exhibits no significant distortion at the end of the simulation, and the total potential energy fluctuates around a constant value, confirming thermal stability at 900 K.

Fig. S2 Thermal stability of (a) Mg_3As_2 and (b) Mg_3SbAs

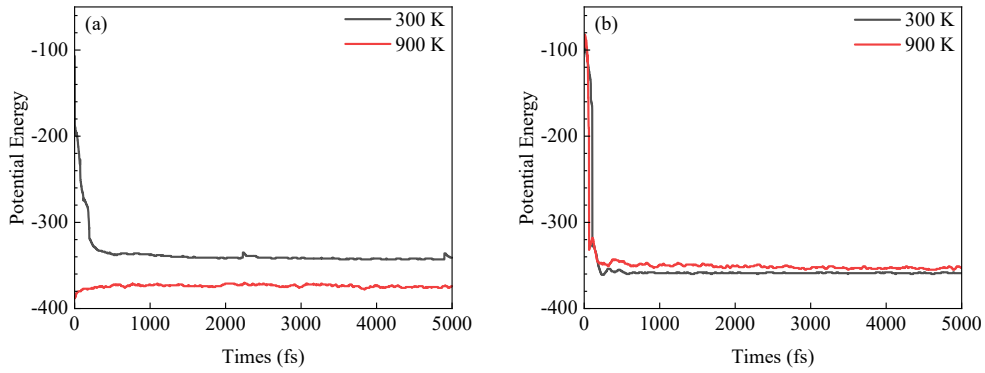

To evaluate the synthesizability of the materials, we calculated the exfoliation energies and compared them with those of the successfully prepared monolayer Mg_3Bi_2.

Table S3 Exfoliation energies of Mg_3SbAs and Mg_3As_2

Matter	Exfoliation Energy
Mg_3As_2	83.2906 meV/Å²
Mg_3Bi_2	52.1932meV/Å²
Mg_3SbAs	64.7775meV/Å²

To accurately describe the lattice thermal conductivity, we performed convergence tests with respect to the interaction range , the q-point sampling density ngrid, and the Gaussian broadening scalebroad, as shown in Fig. S3 of the Supplementary Information. After testing, we decided to use the configuration with scalebroad = 1.5, q-point = 30, and cutoff = 10.

Fig. S3 Convergence tests of (a) Gaussian broadening (broad) and interaction range, (b) q-point grid (ngrid), and (c) interaction range for Mg_3As_2 and Mg_3SbAs

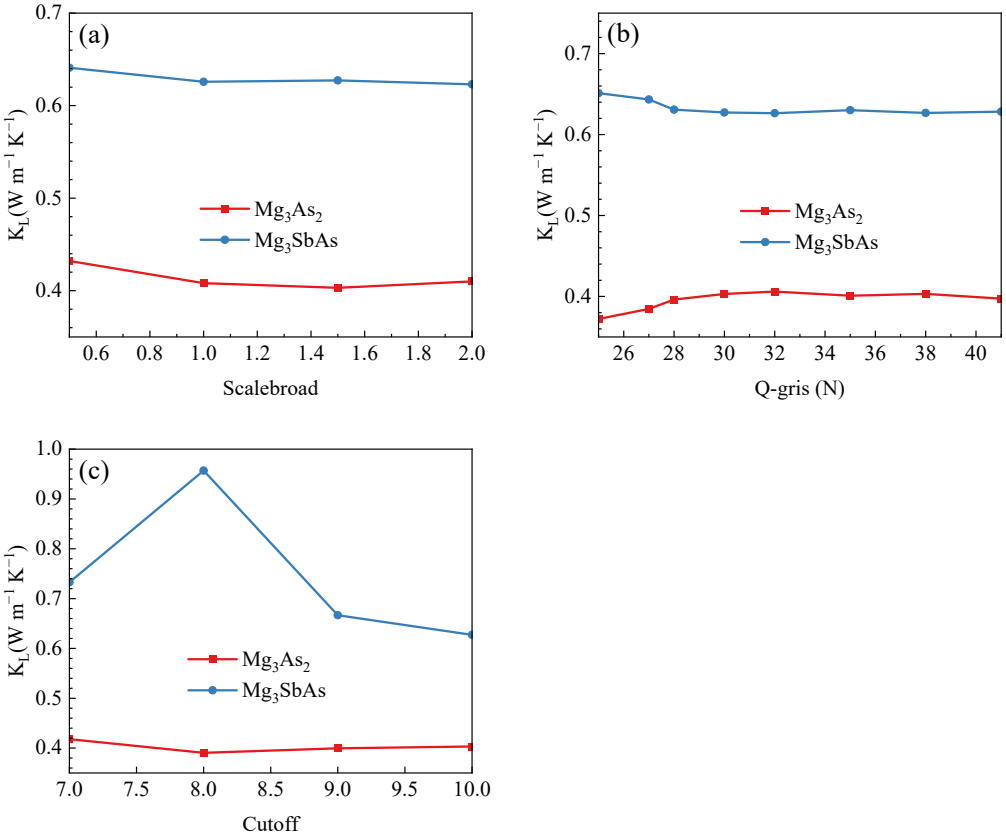

Fig. S4 *zT* values of Mg_3As_2 and Mg_3SbAs at 300 K as a function of carrier concentration

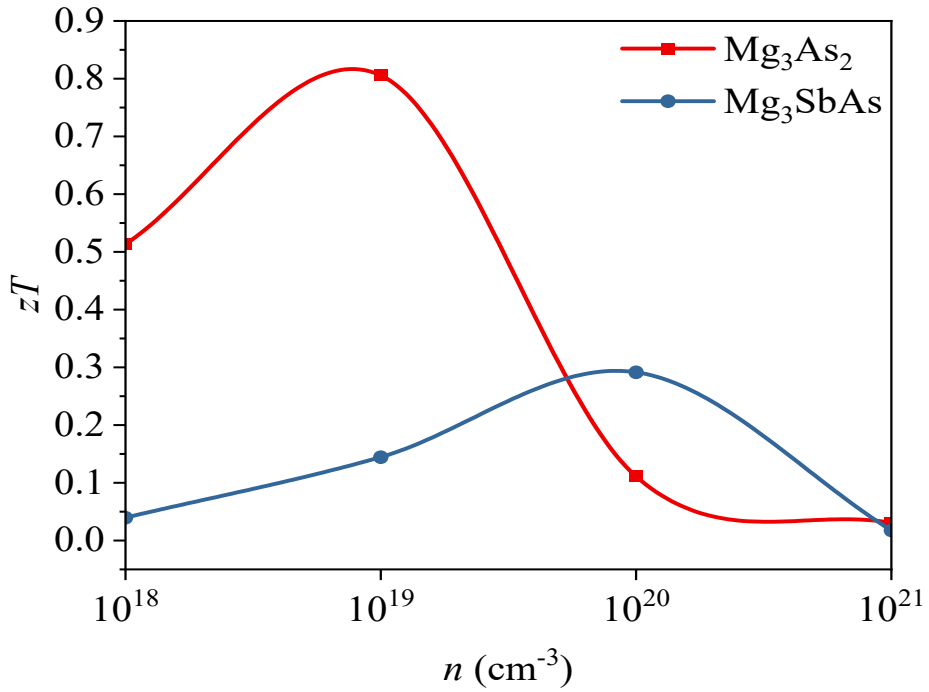

To accurately analyze the bipolar effect of the material, we calculated the intrinsic carrier concentrations at different temperatures. When the intrinsic carrier concentration approaches the doping concentration, the bipolar effect becomes significant; when the intrinsic carrier concentration exceeds the doping concentration, the bipolar effect suppresses the thermoelectric performance of the material.

Table S4 Intrinsic carrier concentration

Temperature(K)	Mg_3As_2	Mg_3SbAs
300 K	8.83×10^{16} cm^{-3}	3.32×10^{12} cm^{-3}
400 K	5.65×10^{17} cm^{-3}	2.27×10^{14} cm^{-3}
500 K	1.85×10^{18} cm^{-3}	3.17×10^{15} cm^{-3}
600 K	4.31×10^{18} cm^{-3}	1.88×10^{16} cm^{-3}
700 K	8.16×10^{18} cm^{-3}	7.15×10^{16} cm^{-3}
800 K	1.35×10^{19} cm^{-3}	1.95×10^{17} cm^{-3}
900 K	2.05×10^{19} cm^{-3}	4.42×10^{17} cm^{-3}

Fig. S5 Variation of electrical conductivity with respect to the CBM, VBM, and band gap E_g for (a) Mg_3As_2 and (b) Mg_3SbAs.